# Instability of geodesic Alfvén modes in rotating tokamak plasmas

A.G. Elfimov
*Institute of Physics, University of São Paulo, 05508-900, São Paulo, Brazil*

Using a quasi-toroidal set of coordinates with coaxial circular magnetic surfaces, drift kinetic equation is solved for collisionless plasmas, and perpendicular dielectric tensor is found for large aspect ratio tokamaks in a low frequency band. Taking into account plasma rotation, and parallel electric field induced by charge separation, it is found that an ion geodesic effect splits Alfvén wave continuum producing continuum minima, which depends on plasma rotation, electron temperature, and poloidal mode numbers at the rational magnetic surfaces. Low frequency geodesic ion Alfvén mode predicted below the continuum minimum has a small collisionless damping for Maxwell distribution of ions. The kinetic ion thermal motion that defines the geodesic effect may drive instability of geodesic modes due to plasma rotation.

## 1. INTRODUCTION

Geodesic Acoustic Modes (GAM) discovered in a theoretical magneto hydrodynamic (MHD) analysis [1] have attracted great interest due to its relevant role on the H-mode and transport barrier (TB) formation to suppress plasma turbulence. The existence of GAMs with $M$= 1, $N$=0 poloidal/toroidal mode numbers was experimentally confirmed [2,3] and many theoretical and numerical investigations are currently being pursued to further understand the characteristics of these mode [4-6]. The formation of the H-mode usually occurs during neutral beam or ion cyclotron resonance heating, which are accompanied by poloidal and toroidal rotation of the plasma column [3]. In a non-rotating plasma, the GAM frequency is $\omega_{GAM}^2 = \omega_s^2(\Gamma + 1/q^2)$ where $\omega_s^2 = \gamma P/(\rho R_0^2)$, $q = rh_\zeta/h_\theta R_0$ is safety factor, $P$ is plasma pressure, $\rho = m_i n_i$ is the mass density, $\gamma$ is the adiabatic index, $R_0$ is the tokamak major radius, $\Gamma$=2 in MHD, and $\Gamma$=7/2 and $\gamma$=1 in kinetic approach [7-10]. The oscillations are electrostatic, which depend on the parallel ($\mathbf{h}\cdot\mathbf{V}$) and binormal ($\mathbf{h}\times\mathbf{e}_r)\cdot\mathbf{V}$ velocities where $\mathbf{h}=\mathbf{B}/B$ and $\mathbf{e}_r$ is radial unit vector, and they have poloidally symmetric radial electric field $E_r$. These oscillations do not perturb the magnetic surfaces ($\delta\mathbf{B}$=0). It has been shown that the flow effect on standard GAM produce a slight up-shift of the frequency [4-6,10] $\omega_{\mathrm{GAM}}^2 \approx \omega_s^2(2 + 1/q^2 + 4V^2/c_s^2)$, as well as for ion-sound geodesic mode $\omega_{GAM\,2}^2 \approx \omega_s^2(1 + 3V_{\mathrm{pol}}^2/c_s^2)/q^2$. Using simplified equilibrium for plasmas with combined poloidal $u_p = u_0[1 - \varepsilon(1+\rho_1)\cos\theta]$ with toroidal $u_t = U + [\varepsilon U - u_0 q(2+\rho_1)]\cos\theta$ rotation along isothermal magnetic surfaces where $\rho_1 = \gamma\left(2M_p^2 - 2M_p M_t + M_t^2\right)\left(1 - \gamma M_p^2\right)^{-1}$, and $M_p^2 = u_0^2/(c_s^2 h_\theta^2), M_t^2 = U^2/c_s^2 << 1$,

and taking into account heat flux we get the dispersion equation [11]

$$\oint R(\nabla\cdot\mathbf{j}_\perp)d\theta = R_0\nabla_r < \mathbf{j} >= \frac{\mathrm{i}\Omega c_s c\rho_0}{B_0 q}\frac{d}{dr}\left[ v_b + \mathrm{i}q\frac{c_s p_s}{\gamma\Omega} + \mathrm{i}q\frac{c_s\rho_s}{2\Omega}M_t^2 + \mathrm{i}\frac{qv_s}{\Omega}M_t \right] = 0$$

The third geodesic or zonal flow (ZF) mode have been found

$$\omega_{ZF}^2 = \left[ M_p^2(1-M_d)^2 + \frac{q^2(\gamma-1)}{2(1+2q^2)}\left(M_t^2 - 2M_t M_p + 2M_p^2\right)M_t^2 \right]\frac{c_s^2}{q^2R_0^2}.$$

The mode frequency stays at the poloidal circulation frequency $u_0/r$ when toroidal rotation $M_t^4 << M_p^2 \sim M_t^2$ is not yet too small. For preferentially toroidal rotation, $M_t^4 >> M_p^2$ we have result of Ref 4. The mode disappears in the formal limit $M_t^2 = 0$.

At the rational magnetic surfaces GAMs may intersect Alfvén wave continuum (AWC), which has frequency $\omega_A = \frac{c_A}{R_0}\frac{B_\zeta}{B}\left(N + \frac{M}{q}\right)$ where $c_A = \frac{B}{\sqrt{4\pi n_i m_i}}$ is the Alfvén speed.

It is very important to verify transitions of the continuum branches and to know where continuum extremum may occur because the real eigenmodes may only propagate at the maximum or minimum of the continuum [6]. In a quasi-cylindrical approach, the AWC equation may be written in the form: $\varepsilon_0\frac{\omega^2R^2}{c^2R_0^2}E_r = \hat{k}_\parallel^2 E_r = \frac{1}{q^2R^2}\left(Nq - \frac{d}{d\theta}\right)^2 E_r$

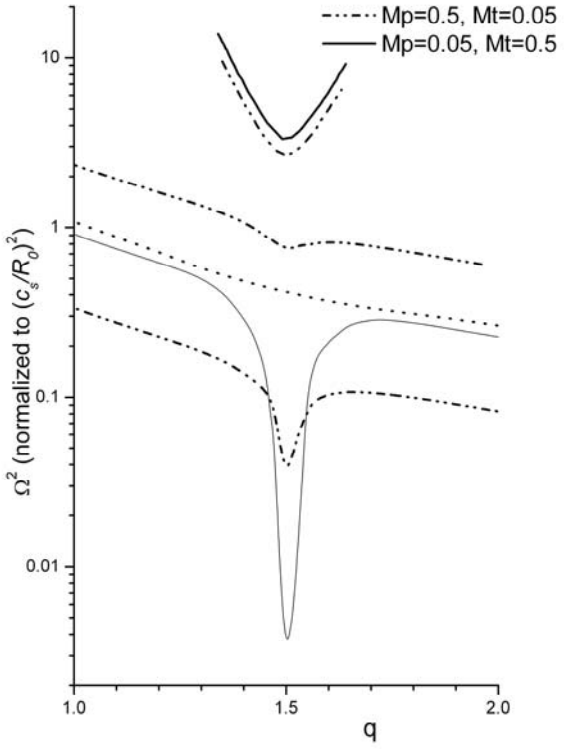


To show transitions between the continuum branches at the rational magnetic surfaces $q=m/n$, the squared frequency of the continuum is plotted schematically in Fig.1 as a function of $q$ at the rational surface defined by $m$=3, $n$=2 poloidal /toroidal mode numbers. Typical tokamak plasma parameters $r=0.1R_0$, $(c_A/c_s)$ =10, and $c/c_A$= *100* are chosen for the preferentially poloidal ($M_p$=*0.5,* $M_t$=*0.05* ) or for preferentially toroidal ($M_p$=*0.05* , $M_t$=0.5 ) rotation. Kinetic studies [8-10] shows existence of GAM like eigenmode at

the extremum of AWC and experimental observations of Alfvén cascades and chirping modes [12-14] generally confirm the theory that may serve as basis of q-profile diagnostics during sawtooth regimes in tokamaks.

Here, we extend MHD study of the rotation effect on GAM and AWC using some kind of a drift kinetic equation [10,15] for low aspect ratio plasmas with circular magnetic surfaces ($R=R_0+r\cdot\cos\theta$, $z=r\cdot\cos\theta$). We calculate a dielectric tensor taking into account ballooning effect, plasma rotation, and the parallel electric field.

The quasi-toroidal set of coordinates ($r,\vartheta,\zeta$) and the cylindrical coordinate system ($v_\perp,\sigma,v_\parallel$) are used where are the normal, angular, and parallel projections on magnetic field lines in the velocity space. The standard drift corrections and flow $V$ along magnetic field in force-free non-compression plasma approach $div\mathbf{V}=0$ are included into equilibrium Maxwell distribution [10,15] for the electrons and ions. The equilibrium balance $\mathbf{j}^*\times\mathbf{B}/c\approx\nabla p$ is provided due to the diamagnetic current where the low plasma pressure $p=p_i+p_e$ is assumed, $8\pi p<<B^2$. The perturbed part of the distribution function, is represented as one wave mode proportional to linear perturbations of the electric and magnetic fields, $f\sim\tilde{E}_{1,2,3},\tilde{B}_{1,2,3}\sim\exp\left(i\left(N_z\zeta-\omega t\right)\right)$ where indexes 1,2,3 indicate the radial, binormal and parallel components. We use the method [10,15] where the $f$-amplitude is expanded into Fourier series over $\sigma$-angle. Taking into account three coefficients of the perturbed distribution, $f=f_0+f_1\cos\sigma+f_2\sin\sigma$, the linearized Vlasov equation is converted into the set of $f_{1,2}$ –equations in the low frequency band $\omega<<\omega_{ci}$. The first order corrections similar to drift kinetic approach is used in $f_0$-equation as $f_1\approx\frac{e}{m\omega_c}\frac{\mathrm{v}_\perp}{\mathrm{v}_\mathrm{T}^2}F_0E_2$, $f_2\approx-\frac{e}{m\omega_c}\frac{\mathrm{v}_\perp}{\mathrm{v}_\mathrm{T}^2}F_0E_1$

$$\left[i\omega-\mathrm{v}_\parallel\left(\frac{h_\vartheta}{r}\frac{\partial}{\partial\vartheta}+iN\frac{h_\zeta}{R}\right)\right]f_0+h_\vartheta\frac{\sin\vartheta}{2R}\mathrm{v}_\perp\hat{L}f_0=\frac{e}{m}\frac{\partial F_0}{\partial\mathrm{v}_\parallel}E_3$$
$$+\frac{e}{2m}\left[h_\zeta^2\frac{\cos\vartheta}{R}\mathrm{v}_\parallel\left(\frac{\mathrm{v}_\parallel}{\mathrm{v}_\perp}-\hat{L}\right)+\frac{\mathrm{v}_\perp}{r}\hat{D}_r\right]\left(\frac{\mathrm{v}_\perp F_0}{\mathrm{v}_\mathrm{T}^2\omega_c}E_2\right) \qquad (1)$$
$$-\frac{e}{2m}\left[\left(\frac{h_\zeta}{r}\frac{\partial}{\partial\vartheta}-iN\frac{h_\vartheta}{R}\right)-h_\zeta\frac{\sin\vartheta}{R}\left(\frac{\mathrm{v}_\parallel^2}{\mathrm{v}_\perp^2}-\frac{\mathrm{v}_\parallel}{\mathrm{v}_\perp}\hat{L}\right)\right]\left(\frac{\mathrm{v}_\perp^2F_0}{\mathrm{v}_\mathrm{T}^2\omega_c}E_1\right)$$

where $\omega_{c\alpha}=\frac{e_\alpha B}{m_\alpha c}$ is the cyclotron frequency, $\hat{L}=\mathrm{v}_\perp\frac{\partial}{\partial\mathrm{v}_\parallel}-\mathrm{v}_\parallel\frac{\partial}{\partial\mathrm{v}_\perp}$ and $\hat{D}_r=\frac{\partial}{\partial r}(r...)$

are operators, $\mathrm{v}_{T\alpha} = \sqrt{T_\alpha / m_\alpha}$ is the thermal speed, $e_\alpha$, $m_\alpha$ are charge, and mass of the plasma species, which are not distinguished due to similarity of equations. To simplify Eq.(1) for electrons, we use quasi MHD approach [10] for typical plasma conditions with the hot electrons, and warm ions $v_{Te} >> \omega R_0 \geq v_{Ti}$. Next, we eliminate $E_3$ from Eq. (1) for ions using the barometric Boltzmann equation for the electrons in the form $\hat{k} f_0 \approx \frac{eF_0}{T_e} E_3$ or $\hat{k}\, \tilde{n}_e = -|e| n_e E_3 / T_e$. Due to plasma quasi-neutrality, we have $f_0^{(e)} \approx F_0^{(e)} \tilde{n}_i / n_i$, and $e_i E_3 = T_e \hat{k}\, \tilde{n}_i / n_i$ where $\hat{k} = \frac{1}{R}\left( \frac{h_\vartheta}{r} \frac{\partial}{\partial \vartheta}(R...) + \mathrm{i} N h_\zeta \right)$ is the parallel operator. Now, the electron part is eliminated and the perturbed ion distribution function is divided into cylindrical and toroidal parts, $f_0^{(i)} = f_i^{\mathrm{cyl}} + \tilde{f}^{(i)}$, where drift effect may be kept in cylindrical part [11] but cross corrections with drift are ignored in the toroidal part due to $\omega^* << \omega$. After Fourier series $\tilde{f}^{(i)} = \sum_M f_M^{(i)} \exp(\mathrm{i} M \vartheta)$ we get

$$
\begin{aligned}
\tilde{f}_{M\pm1}^{(i)} &= \frac{T_e F_0^{(i)}}{T_i n_i} \frac{(\mathrm{v}_\parallel - V_0) k_{M\pm1}}{\left(\omega - \mathrm{v}_\parallel k_{M\pm1}\right)} \tilde{n}_{M\pm1} \pm \frac{h_\vartheta}{4 R_0 \mathrm{v}_{\mathrm{Ti}}^2} \frac{\mathrm{v}_\perp^2 V_0 - 2\mathrm{v}_\parallel \mathrm{v}_{\mathrm{Ti}}^2}{\left(\omega - \mathrm{v}_\parallel k_{M\pm1}\right)} f_M^{\mathrm{cyl}} \\
&- \frac{e_i}{4 m_i} \frac{F_0^{(i)} E_{1,M}}{\mathrm{v}_{\mathrm{Ti}}^2 \omega_{c0}} \frac{h_\zeta}{R_0} \left[ \frac{\mathrm{v}_\perp^2 (M \pm 1)[\mathrm{v}_{\mathrm{Ti}}^2 - V_0(\mathrm{v}_\parallel - 2V_0)] \pm \mathrm{v}_\parallel (2\mathrm{v}_\parallel \mathrm{v}_{\mathrm{Ti}}^2 - V_0 \mathrm{v}_\perp^2)}{\left(\omega - \mathrm{v}_\parallel k_{M\pm1}\right) \mathrm{v}_{\mathrm{Ti}}^2} \right] \\
&- \mathrm{i} \frac{e_i}{4 m_i} \frac{h_\zeta^2 \mathrm{v}_\parallel (2\mathrm{v}_\parallel \mathrm{v}_{\mathrm{Ti}}^2 - V_0 \mathrm{v}_\perp^2) + \mathrm{v}_\perp^2 [\mathrm{v}_{\mathrm{Ti}}^2 - V_0(\mathrm{v}_\parallel - 2V_0)] \left(1 + \hat{D}_r\right)}{\omega_{c0} R_0 \mathrm{v}_{\mathrm{Ti}}^2 \left(\omega - \mathrm{v}_\parallel k_{M\pm1}\right)} \left( \frac{F_0^{(i)} E_{2,M}}{\mathrm{v}_{\mathrm{Ti}}^2} \right)
\end{aligned}
\qquad (2)
$$

where $f_M^{\mathrm{cyl}} \approx -\frac{e_i}{2 m_i} \frac{\mathrm{v}_\perp^2}{\omega \omega_{c0}} \left[ \mathrm{i} \hat{D}_r \left( \frac{F_0^{(i)} E_{2,M}}{\mathrm{v}_{\mathrm{Ti}}^2} \right) + M \frac{F_0^{(i)} E_{1,M}}{\mathrm{v}_{\mathrm{Ti}}^2} \right]$, $k_M = M h_\vartheta / r + N h_\zeta / R_0$ is the parallel wave number. The Eq. (2) is valid at the rational surfaces where $k_M \approx 0$ and two sideband harmonics ($M \pm 1$) in the relation to the main harmonic $M$ are only taken into account due to the approximation $r^2 << R^2$. Then, integrating Eq. (2) in the velocity space, we get the equation for the geodesic ion density perturbation as follows:

$$
\frac{\tilde{n}_{M\pm1}}{n_{\mathrm{i}}} = \frac{e_i h_\zeta}{m_i R \omega_c \omega} \chi_{M\pm1} \left( \pm \tau_{M\pm1}^{(1)} E_{1,M} + \mathrm{i} \hat{\tau}_{M\pm1}^{(2)} E_{2,M} \right) \qquad (3)
$$

where $\chi_{M\pm1} = \left[ \frac{T_i}{T_e} + \left(1 + z_{M\pm1} Z(z_{M\pm1})\right) \right]^{-1}$, $z_{\pm1} = \frac{(\omega - V k_{M\pm1})}{\sqrt{2} \mathrm{v}_{\mathrm{Ti}} k_{M\pm1}}$, $k_{M\pm1} = \frac{\pm 1}{R_0 q_s}$,

$w_0 = \frac{V_0}{\sqrt{2} \mathrm{v}_{\mathrm{Ti}}}$, $Z(z_{\pm1}) = \frac{1}{\sqrt{\pi}} \int_{-\infty}^{\infty} \frac{dt \exp(-t^2)}{(t - z_{\pm1})}$ is the dispersion function, $z_{M\pm1} = \zeta_{M\pm1} - w_0$

$$\tau_{\pm 1}^{(1)} = \left[ \left( (z_{M\pm1}^2 + \frac{1}{2})\zeta_{M\pm1} + z_{M\pm1} w_0^2 \pm M(1 - z_{M\pm1}^2) w_0 \right) Z(z_{M\pm1}) \right]$$

$$+ z_{M\pm1}(\zeta_{M\pm1} \mp M w_0) \mp M\left(\frac{1}{2} + w_0^2\right)$$

$$\hat{\tau}_M^{(2)} E_{2,M} = \left[ z_{M\pm1} + \left(\frac{1}{2} + z_{M\pm1}^2 + w_0^2\right) Z(z_{M\pm1}) \right] \zeta_{M\pm1} E_{2,M}$$

$$+ \hat{D}_r \left[ \left( \frac{1}{2} + w_0 \zeta_{M\pm1} + w_0 (z_{M\pm1}^2 - 1) Z(z_{M\pm1}) \right) E_{2,M} \right]$$

After inserting of the $\tilde{f}_{M\pm1}^{(0e,i)}$ functions into the $\tilde{f}_{1,2}$–equations taken from Ref 10, which have to be averaged over magnetic surface taking into account the ballooning effect, and integrating in the velocity space we get the tensor corrections

$$\sum_p \tilde{\varepsilon}_{sp} E_{p,M} = \frac{4\mathrm{i}\pi^2}{\omega} \sum_{e,i} e_i \int_{-\infty}^{\infty} dv_\perp v_\perp^2 \int_0^{\infty} dv_\parallel \oint \left(1 + \frac{r}{R}\cos\vartheta\right) f_s d\vartheta . \qquad (4)$$

To proceed with the mode analyses, we use the approach [10,15] based on Hain-Lust eigenmode equation, which is reproduced here to understand following discussion,

$$\frac{d}{dr}\left( rD \frac{dF}{dr} \right) + \left[ \frac{dQ}{dr} - \frac{M^2 D}{r} \right] F = 0 \qquad (5)$$

where $F = rE_b$, $Q = \left[ M\, {2k_M}/{R_0 q} + M\, {\omega_{ci}}/{c_A^2} \left( \omega_i^* - \omega_e^* \right) \right]$, and the AWC equation has the form $D = \frac{\omega^2}{c^2}\left( \varepsilon_{11}^0 + \tilde{\varepsilon}_{11} - M^2 \tilde{g}_{22} - M\tilde{g}_{12} - M\tilde{g}_{21} \right) - k_M^2 = 0$. Eq. (5) is valid in the approximations typical for large aspect ratio tokamaks, $\tilde{\varepsilon}_{11} >> \tilde{g}_{21}\tilde{g}_{12} r^2 \frac{\omega^2}{c^2}$, $M^2 >> r^2\, {\omega^2}/{c_A^2}$, which help to reduce number of terms in coefficient in the front of the first derivative. Drift parts of the $\varepsilon_{11}, \varepsilon_{22}$ cylinder tensor components in Eq. (A5) of Ref 15 are small in comparison with geodesic part but the drift parts in the $\varepsilon_{12}^{cyl}, \varepsilon_{21}^{cyl}$ tensor components are large than the geodesic parts, $\omega^* \omega_{ci} >> \omega^2 >> \omega\omega^*$. Using these approximations, we present parts of the high complexity tensor components in Appendix (A1-A4), which are only necessary for the continuum equation,

$$D = \frac{\omega^2}{c^2}\left( \frac{c^2}{c_A^2} + \varepsilon_{11}^{\mathrm{geo}} \right) - k_M^2 = 0, \quad \varepsilon_{11}^{\mathrm{geo}} = -\sum_{i,e} \frac{\omega_{pi}^2 h_\zeta^2 \mathrm{v}_{\mathrm{T}i}^2}{\omega_{ci}^2 R^2 \omega^2} \Psi(\zeta) \,, \zeta = \frac{R_0 q \omega}{\sqrt{2}\mathrm{v}_{\mathrm{Ti}}}. \qquad (6)$$

where the geodesic function has the form:

$$\Psi(\zeta) = -\chi\zeta\left(\zeta^2 Z + \frac{1}{2}Z + \zeta\right)\left(2 + 2\zeta^2 + \zeta(1+2\zeta^2)\right)Z$$
$$- M\chi\left[\left((\zeta^2-1)\zeta Z + 3\zeta^2 - \frac{3}{2}\right)Z + 2\zeta\right]w_0$$
$$- 2\chi\zeta\left[\left(8\zeta^6 - 6\zeta^4 - 4\zeta^2 + \frac{1}{2}\right)\zeta Z^2 + \left(1 - 9\zeta^2 - 6\zeta^4 + 16\zeta^6\right)Z + 4\zeta(2\zeta^4 - 1)\right]w_0^2 \qquad (7)$$
$$+ Z\zeta\left(3 + 4t_e - \zeta^2(6t_e + 4) + (4t_e - 6)\zeta^4 + 4\zeta^6\right)w_0^2 - 4\zeta^2\left(1 + t_e + (1-t_e)\zeta^2\right)w_0^2$$
$$+ \zeta\left[\left(1 + t_e + 2\zeta^2 + 2t_e\zeta^2 + 2\zeta^4\right)Z + \zeta(2\zeta^2 + 2t_e + 3)\right]$$

where $t_e = T_e/T_i$, and $\chi = \left[1/t_e + \left(1 + \zeta Z(\zeta)\right)\right]^{-1}$. In second order of the cold ion limit, $|\zeta - w_0|^2 >> 1$, the geodesic function can be presented in the form:

$$\Psi(\zeta) = 7/2 + 2t_e + 4(1+t_e)w_0^2 + 2(a+t_e)/\zeta^2 + 4t_e/(2\zeta^2 - t_e) \qquad (8)$$

where $a$ depends on number of terms taken in $Z(\zeta)$-asymptotic expansion ($a$=1for three terms, and $a$=23/8 for four terms and that result is similar to the one in Ref 9). In this case, upper branch of the Alfvén continuum $\omega_A = \sqrt{(c_A k_M)^2 + \omega_{geo}^2}$ has the minimum at $k_M$=0 defined by the frequency $\omega_{\mathrm{GIAM}}^2 \approx \left[\frac{3}{2} + 2\left(1 + \frac{T_e}{T_i}\right)\left(1 + \frac{V_0^2}{\mathrm{v}_{\mathrm{Ti}}^2}\right) + \left(a + \frac{T_e}{T_i}\right)\frac{1}{q^2}\right]\frac{\mathrm{v}_{\mathrm{Ti}}^2}{R_{\mathrm{Ti}}^2}$

where approximation $\zeta^2 \approx 2q^2 >> 1$ is used. This frequency is valid as an approximate value and numerical calculations of Eq. (8) have to be used to obtain a correct value. The low branch of the continuum appears at $\omega_{GIS}^2 \approx \frac{T_e(1-\delta)}{m_i R_0^2 q^2}$, $\delta \approx \frac{4T_e(T_e+4)}{23T_i^2 + 7T_iT_e + 4T_e^2}$ in Eq. (8) , which is related to the ion sound geodesic mode [8,10,13]. We note that dependence on the plasma rotation is similar to MHD approach [4, 11]. The result for $V_0$=0 generally coincides with [7-9, 13] in the respective conditions, and differs in numerical coefficients from our previous [15] due to averaging procedure in Eq. (4). The numerical analyzes of Eq. (7) show that two branches of $\mathrm{GAM}_{1,2}$ are jointed at $q$=0.8-0.9 for comparable values of electron and ion temperatures. It should be noted that the GAM frequency is obtained as some limit of the AWC theory for each rational surface $q$=-$M/N$. In Fig.2, to demonstrate importance of the kinetic effects, the GAM and continuum frequencies are plotted for different values of the velocity ($V/\mathrm{v}_{\mathrm{Ti}}$=-0.28 and -0.56) as function of $q$, which variation may simulate the radial dependence of the modes in tokamak for the monotonic q-profile. The frequencies are normalized to the ion circulation frequency $v_{Ti}/R_0$. In the figure, we can observe two branches of continuum

lines at q=2: the upper branch is related to the AWC and the ion-sound continuum (ISC) $\omega_{IS}^2 \approx T_e/(m_i R_0^2 q^2)$ appears below the one. The calculations of $GAM_{1,2}$ frequency show that there is an threshold for the modes at $q_{th}\approx 0.85$ for electron temperature approximately equal to the ion one ($T_e=1.2\ T_i$). It means that there are no GAMs for $q<q_{th}$ as it shown in Fig.2 and the AWC minimum frequency may strongly jump "up" or "down" at the $q$-threshold. The calculations show that the threshold is monotonically diminuend to $q_{th}\approx 0.6$ when the electron temperature grows to $T_e\approx 2\ T_i$. We note that that the continuum curves in Fig.2 moves left and up with electron temperature increasing.

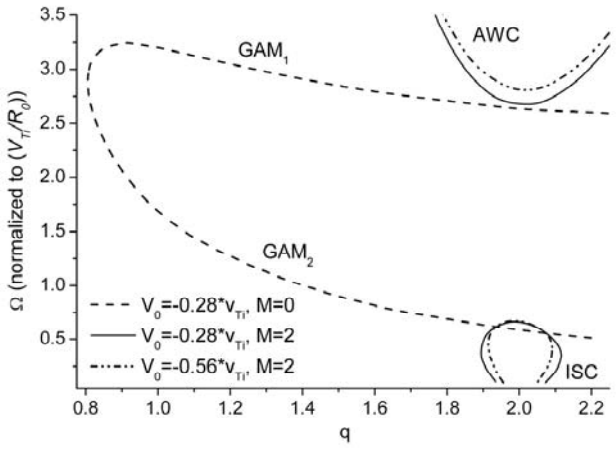


*Fig.2.Plot of the geodesic frequency for M=0, AWC and ISC for M=2 as the function of q-factor for different $V=0.28v_{Ti}$ (solid line) and $V=0.28v_{Ti}$ (chain line) where frequency are normalized on the ion circulation frequency . The temperature ratio is $T_e/T_i=1.1$ and typical tokamak plasma parameters $(c_A/c_s)=10$, and $c/c_A=100$ at $r=0.1R_0$, are chosen, which are the same as in Fig.1.*

Due to rotation, the continuum begins to depend on $M$-number and the rotation parameter $\Omega = VR_0 h_\vartheta / rh_\zeta$, whose effect is related to the poloidal part of the velocity. Due to kinetic effects, there is strong variation of the $GAM_2$ and IS continuum with changing of the sign of the parameter $M\Omega$. Generally, the $GAM_1$ dispersion curve moves up and left with increasing the rotation speed. For $M\Omega=const$, the GAM curves appear as the same. For counter rotation $M\Omega<0$, curves moves higher up in comparison with $M\Omega>0$ but the difference between the positive and negative rotation is very small for the AWC branch. The ISC branch is strongly modified for $M\Omega>0$. The ion sound continuum has maximum at the rational surface in the case of counter rotation but the mode disappears for co-rotation that may transforms to the rotation branch discussed in Refs 6 and 11.

Basing on analysis of Eq. (5) it should be noted that the eigenmode formation at the continuum extremum depends strongly on the relation between gradients of plasma pressure and the magnetic shear [10-13]. When the plasma pressure gradients are strong, the AE may propagate at the maximum of the AWC; however, if the pressure gradients

are weak and the magnetic shear large, the modes may appear at AWC minimum ($\omega = \omega_{geo} - \delta\omega$ and $\delta\omega << \omega_{geo}$) where geodesic frequency should be calculated using Eq. (7). The real part of the geodesic function is used in Eq. (8) because the imaginary part is not important to obtain the continuum equation (7). The imaginary part of the geodesic function taken from Eq.(7) is exponentially small for the AWC branch, $\mathrm{Im}\,\Psi \approx \sqrt{\frac{\pi}{2}}\left[ |Mq| \frac{\omega R_0}{2\mathrm{v}_{\mathrm{Ti}}} \frac{T_e}{T_i} - \frac{V_0}{\mathrm{v}_{\mathrm{Ti}}} \left( \frac{\omega R_0 q}{\mathrm{v}_{\mathrm{Ti}}} \right)^4 \right] \exp\left[ -\left( \frac{\omega R_0 q}{\sqrt{2}\mathrm{v}_{\mathrm{Ti}}} \right)^2 \right]$ that begins to be large for the ion-sound branch, $\mathrm{Im}\,\Psi \approx M \frac{T_e}{T_i} \delta\zeta^3 \exp(-\zeta^2) \left| \delta - \mathrm{i} \frac{T_e}{T_i} \sqrt{\pi} \zeta^3 \exp(-\zeta^2) \right|^{-2}$ GAE may be unstable for the low poloidal numbers, $\frac{V_0}{\mathrm{v}_{\mathrm{Ti}}} > |M| \frac{T_e}{2T_i} \left| \frac{\mathrm{v}_{\mathrm{Ti}}}{\omega R_0 q} \right|^3$.

Finally, we conclude that the kinetic approach developed in the paper shows that the minima of the Alfvén and ion-sound continua are defined by the geodesic effect of the plasma ions, and can be modified by the plasma rotation at the rational magnetic surfaces. The MHD limits obtained from that approach stays mainly in accordance with published results. The geodesic effect has the q-minimum threshold defined by the electron temperature or the plasma rotation. The geodesic ion Alfvén modes may be driven by rotation below or above of the continuum minimum like some global mode.

Author is thankful to CNPq (National Council of Brazil for Science and Technology Development) for financial support.

[1] Winsor N, Jonson J L, Dowson J M, (1968) *Phys. Fluids*, 11, 2448.

[2] Krämer-Flecken A, *et al*, 2006 *Phys. Rev. Lett.* **97**, 045006.

[3] Conway G D *et al*, 2005 *Plasma Phys. Control. Fusion*, **47**, 055009.

[4] Wahlberg C (2008) *Phys. Rev. Lett*. 101, 115003

[5] Ilgisonis VI *et al*, 2011 *Plasma Phys. Control. Fusion*, **53,** 065008.

[6] Haverkort J W *et al*, 2011 *Plasma Phys. Control. Fusion*, **53,** 045004.

[7] Zonca F, and.Chen L and Santoro R. A. 1996 *Plasma Phys. Control. Fusion*, **38**, 2011,.

[8] Smolyakov AI, Nguyen C, Garbet X, (2008) *PPCF*, 50, 115008

[9] Lauber P, Brudgam M, Curran D et al. (2009) *PPCF*, 51, 124009.

[10] Elfimov AG, (2010) *Physics of Plasmas* **17**, 022102.

[11] Elfimov AG *et al*, (2011) *Plasma Phys. Control. Fusion,* **53,** 105003

[12] Elfimov AG, (2010) *Physics of Plasmas* **17,** 110705

[13] Elfimov A.G. et al. (2011) *Plasma Phys. Control. Fusion,* **53**, 025006

[14] Gorelenkov N N et al., 2007 *Plasma Phys. Control. Fusion,* 49 B371-B383

[15] Elfimov A.G. *et al*, (2008) *Phys. Plasmas* **15**, 074503